

# Synchronous reference frame DQ current control for single phase grid connected cascaded H bridge multilevel inverter

V. S. Kirthika Devi <sup>1\*</sup>, S. G. Srivani <sup>2</sup>

<sup>1</sup> VTU Research Scholar, Faculty, Department of Electrical and Electronics Engineering

<sup>1</sup> Amrita School of Engineering, Bengaluru, Amrita Vishwa Vidyapeetham, India

<sup>2</sup> Department of Electrical and Electronics Engineering, R V College of Engineering, Bengaluru

\*Corresponding author E-mail: [kirthika.rajesh15@gmail.com](mailto:kirthika.rajesh15@gmail.com)

## Abstract

The main focus on this paper deals with a current control technique for the inverter using a PV system for grid connected topology. The work of this paper is to evolve the PV model by tracking maximum power point using Incremental conductance algorithm by applying synchronous reference frame control method for single phase transformer less cascaded H Bridge Multilevel Inverter via boost converter system connected to 230V grid. A Phase shifted pulse width modulation technique is also projected in order to afford the pulse for voltage source inverter. The mathematical expressions for the control design for the single phase system is expressed in this paper. The analysis of the control is adopted using PI control method and is executed in synchronous rotating d-q reference frame in order to carry out the response of the best output voltage for the grid connected single phase PV system. The d-q technique is applicable only for the three phase system due to the minimum requirement of two independent phases. Hence one quadrature phase inverter is added additionally in the control method. The simulation is done using MATLAB/SIMULINK.

**Keywords:** Photovoltaic Module; Incremental Conductance; Boost Converter; Cascaded H Bridge Multilevel Inverter; PI Controller; MPPT; Phase Shifted Pulse Width Modulation; D-Q Synchronous Reference Frame; Total Harmonics Distortion; Efficiency.

## 1. Introduction

Among the non-conventional energy sources photovoltaic model is mostly influenced due to its pureness, reduction in the cost of the fuel and due to its less maintenance. Even though its initial cost is high. Primarily when this solar is used it has couple of issues: A PV module which functions with rigid temperature and radiation provides a nonlinear P-V Characteristics which gives the maximum power point afford the enormous desirable output power under specific environment condition [1]. The efficiency of the solar array will be depressed and hence the generation of the power by solar cells changes with change in temperature and irradiance [2] & [3]. In the latest years, a huge number of MPPT techniques have been suggested and carried out [4]. Amongst all MPPT method Incremental conductance algorithm provides the fast response [5] - [8]. The output of the DC from the PV is connected to the DC-DC converter [9]-[11].

The power will be delivered to the grid and even to the local loads for the Grid-connected system. Designing a relevant current controller using a phase locked loop (PLL) for synchronizing with grid [12] & [13] is a very big effort. Generally Synchronous frame regulators(SRF)are acknowledged to have a superior achievement than the stationary frame regulators [14]. SRF using three phase current controller in a d-q frame is possible but in a single phase system it is very challenging task to produce zero steady state error at grid frequency. Hence the SRF control exists in converting an orthogonal pair that is self-assured by certain single phase input current and an imaginary current into a rotating frame from a stationary frame control [15],[16].An inverter which is commonly used for single

phase system is the full bridge inverter. The multilevel inverter (MLI) plays an extensive role and is well applicable for several renewable sources such as solar, Fuel cells, wind etc. MLI is of three types flying capacitor, neutral point clamping and cascaded h bridge MLI. Amongst these three methods cascaded h bridge plays an important role for high and medium power applications even though it has one disadvantage of having many dc sources in it depending upon number of levels [17] & [18], but it is suitable for applying hybrid renewable sources. The pulses given to the inverter switches are of several types as explained in [19] – [21]. For the PV inverter grid connected system the most accepted control design for the grid inverter is a current controlled cascaded H bridge PWM with low pass filter at the output stage. The most common trend nowadays is to adopt the LCL filter design due to its compact design [22]. Omission of transformers also eases out cost pressure, improves affordability and makes it convenient to the users when the inverter is integrated with the grid connected system [23]-[25].

The main aim of this paper is by presenting a single phase PV system for a dual stage converter topology. MPPT technique using incremental conductance algorithm is used for tracking maximum power from the solar arrays. The PV output is connected to a DC-DC boost converter in order to increase the input voltage level to the required output voltage this is connected using a DC link capacitor. The LCL filter design is used which eradicates the ripples that has been created due to high frequency and is given to the grid. The voltage from the grid and the inverter current are given to the current controller in order to regulate the supply current. The Phase locked loop(PLL) is used for tracking the grid voltage angle ( $\omega t$ ). The error signal is compensated with the help of the PI controller

using the synchronous reference frame current control method and that develops the reference signal to the modified phase shifted PWM technique which in turn generates the switching pulses for the grid connected single phase inverter system.

## 2. System description

The proposed system is applied with four control strategy that includes firstly the PV system with IC MPPT control algorithm; the pulse generated by this is given to the boost converter switch. Secondly a modified phase shifted pulse width modulation control technique given to the transformer less single phase cascaded H bridge inverter switches, and thirdly the synchronous reference frame (SRF) current controller where the grid voltage and the current from the inverter used for controlling the supply current. The LCL filter is used in order to suppress the harmonics developed by the high frequency. The phase angle is developed by the grid voltage with the help of the PLL. This SRF current control alone the flaws signal with the aid of PI controller and develops the reference signal which is used to generate the pulses for the inverter switches with the help of PSPWM technique. The entire block diagram is shown in Fig.1.

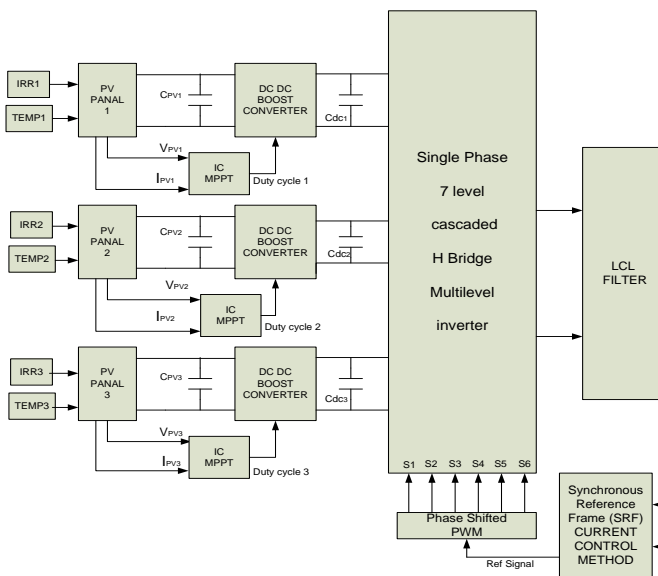


Fig. 1: Block Diagram for the Proposed System.

## 3. Designing and analysis of the proposed system

### 3.1. The mathematical model of an ideal PV

The photovoltaic ideal model is shown in Fig.2. The expression from the theory of semiconductors [4] provides the V-I characteristics curve of the photovoltaic and the mathematical expression is given in equation (1) and (2).

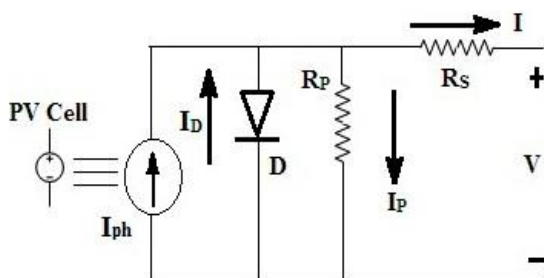


Fig. 2: Equivalent Circuit of A Solar Cell.

I-Output cell current, ki-Current Co-efficient, RS-Series Resistance, kV-voltage coefficient, IPV-Photovoltaic current, Vt-Thermal voltage, V-Output cell voltage, T-Cell temperature in oC, q-Electronic charge [1.60217646\*10<sup>-19</sup>C], K-Boltzmann's constant [1.3806503X10<sup>-23</sup>J/K], IO-Saturation current, RP-Parallel

$$I = I_{pv} - I_0 \left[ \exp\left(\frac{V + I * R_s}{V_t * a}\right) - 1 \right] - \frac{V + I * R_s}{R_p} \quad (1)$$

Resistance, Tr-Reference temperature, Ior - Saturation Cell current at Tr, ISC -Short-circuit current at 25°C and 1000 W/m2. The P-V curve is shown in Fig. 3 (a) and the I-V Characteristic curve is shown in Fig.3 (b).

$$I_0 = \frac{I_{sc,n} + K_1 * \Delta T}{\exp\left(\frac{V_{oc,n} + K_V * \Delta T}{a * V_t}\right) - 1} \quad (2)$$

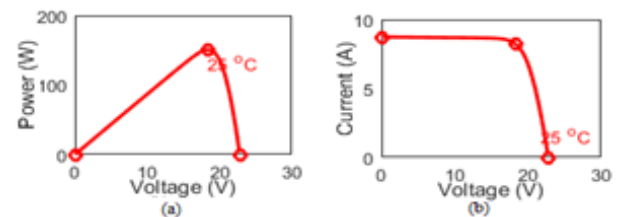


Fig. 3: A) Power vs. Voltage B) Current vs. Voltage Curve.

### 3.2. Boost (DC-DC) converter

In this paper boost method dc-dc converter is utilized and the pulse for the switch is taken from the IC algorithm where the maximum power is tracked and the duty cycle is obtained. The boost converter is shown in Fig.4. [9]-[11]. The duty cycle (D) is calculated as shown in the below expression

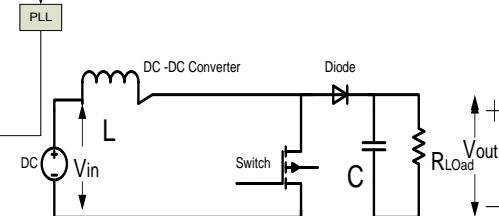


Fig. 4: Circuit Diagram of Boost Converter.

$$\frac{V_{out}}{V_{in}} = \frac{1}{1-D} \quad (3)$$

The inductor value for the boost converter is calculated using the expression (4)

$$L = \frac{(V_{in}) * D}{(\Delta i_L) * f} \quad (4)$$

The capacitance value is calculated by

$$C = \frac{(V_{out}) * D}{(\Delta V_{out}) * f * R_{Load}} \quad (5)$$

Rload is calculated using (Vout) 2/Pinput, where the VIN is 18.4V, Iin is 8.2 A, Pm is 150.88W. The Calculated C is 52µF,L is 260µH, ΔiL is assumed to be 40% and ΔVout is assumed to be 1% . The Rload is 80.2Ω.

### 3.3. Cascaded H bridge multilevel inverter

In high and medium power applications Cascaded H Bridge (CHB) multilevel inverter plays a very important role. This resides number of series H Bridge where every H Bridge has independent DC source. Renewable sources such as solar, wind, fuel cells, battery can be replaced instead of each Dc source. In this paper 7level is considered. The levels are calculated with expression  $2N+1$ . Here N denotes the number of levels. This causes seven different output voltages such as +3Vdc, +2Vdc, +1Vdc, 0, -1Vdc, -2Vdc, and -3Vdc. The seven level cascaded H Bridge is shown in Fig.5. In this paper instead of DC source PV module is used.

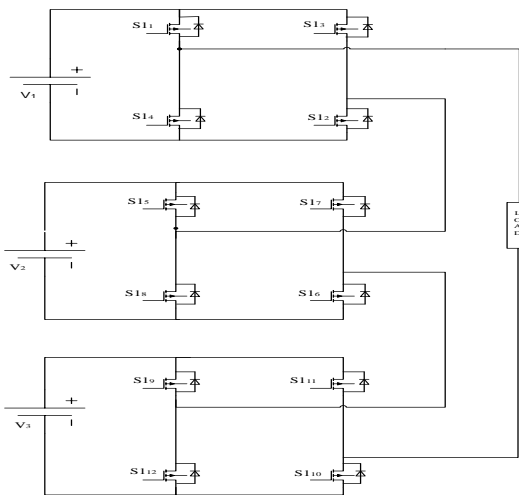


Fig. 5: Circuit Diagram of Cascaded Seven Level H Bridge Multilevel Inverter.

### 3.4. Design of DC link capacitor

The DC link capacitor is utilised as an energy storage load balancing device. This capacitor is placed between the DC and the AC of the voltage source inverter. This element helps by securing the inverter circuit from temporary electromagnetic interference voltage spikes and surges. DC link capacitor is a necessary element to accomplish the appropriate performance of the system.

The DC link capacitor for PV is calculated using the expression (6).

$$C_{pv} = \frac{V_{pv} * D}{4 * L_{dc} * \Delta V_{pv} * f_{dc}^2} \quad (6)$$

Where,  $V_{pv}$  is the PV voltage used in this system.  $D$  is the duty cycle of the boost converter.  $\Delta V_{pv}$  is the 2% of the PV voltage obtained by the solar panel of single H-Bridge converter  $f_{dc}$  is the converter frequency and  $L_{dc}$  is the converter inductor value. The DC link capacitor between the boost converter and the inverter is calculated using expression (7). The calculated  $C_{pv}$  value is 100 $\mu$ F.

$$C_{dc} = \frac{P_{max}}{2 * \omega_{grid} * V_{ripple} * V_{dc}} \quad (7)$$

Here,  $P_{max}$  is the output maximum power of boost dc-dc converter for each PV,  $V_{dc}$  is the voltage output of boost converter, and ' $\omega_{grid}$ ' is grid frequency  $V_{ripple}$  represents the peak of the voltage at MPP and it is considered to be less than 6% of the MPP voltage and for the proposed system it is considered as 2.5%. The calculated  $C_{dc}$  value is 4748  $\mu$ F.

## 4. Control methods used for the proposed system

The control techniques used in this system is categorized as four different schemes. Firstly, Incremental conductance MPPT algorithm. Secondly the phase shifted pulse width modulation (PWM). Thirdly the synchronous reference frame (SRF) current control is used along with the PI controller in order to develop the reference sine signal for the inverter switches. and lastly the filter design is used which helps in reducing the noise that are usually created by means of the inverter circuit. In this paper LCL filter is adopted.

### 4.1. Incremental conductance MPPT control technique

The characteristics curve depends on to the irradiance level and also on the temperature of the PV cell. The slope of the PV curve with respect to power  $dP/dV$  at the MPP is zero and it fewer on the right-hand of the MPP and increments on the left-hand part of the MPP.

$$\frac{dI}{dV} = -\frac{I}{V} \text{ at MPP} \quad (8)$$

$$\frac{dI}{dV} > -\frac{I}{V} \text{ at Left MPP} \quad (9)$$

$$\frac{dI}{dV} < -\frac{I}{V} \text{ at right MPP} \quad (10)$$

The flowchart of the IC is shown in Fig.6. In this algorithm the accurate value is obtained with very less oscillation at the maximum power point. The duty cycle from the algorithm is compared with the repeating sequence and the pulse is given to the boost converter switch. This method tracks the maximum power and gives better efficiency when compared with the other MPPT algorithms.

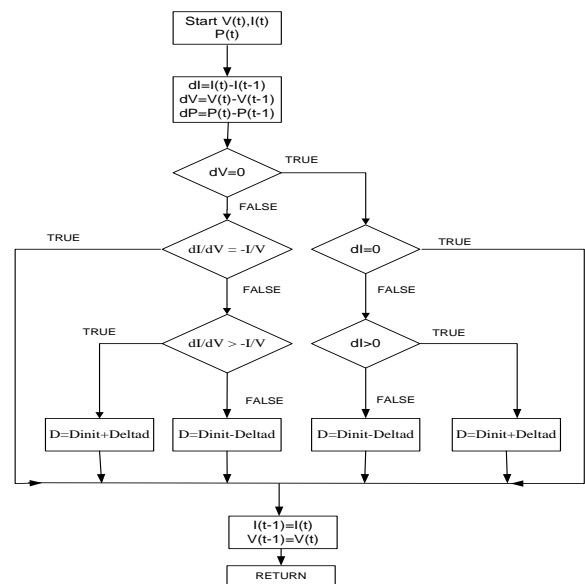


Fig. 6: Flowchart for the IC MPPT Algorithm.

### 4.2. Designing of modified phase shifted PWM strategy

The PWM technique used in this system is a modified phase shifted method. This system consists of a signal carrying 120° phase difference between 3 carrier waves, the peak value is taken as 1 for all the three sets of carrier signals that is from 0 to 1 in positive side, and from 0 to -1 is for negative cycle which will be exactly 180° difference with respect to the positive side. The pulses are generated using the bipolar reference sine wave compared with the modified carrier signal technique. The carrier wave signals are picked using

the equation  $(n-1)/2$ . The reference sine wave signal is then compared with each of the carrier triangular wave where each signal phase difference is calculated using the expression  $360/((n-1)/2)$ . The carrier waves and reference wave is shown in Fig.7.

$$\begin{bmatrix} I_d \\ I_q \end{bmatrix} = \begin{bmatrix} I \cos \phi \\ I \sin \phi \end{bmatrix} \quad (16)$$

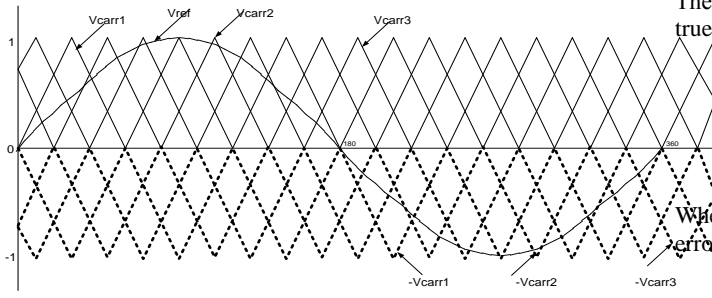


Fig. 7: The Modified Phase Shifting Pulse with Modulation.

The phase angle  $\Phi$  is considered to be 0 ( $\Phi=0$ ) in order to supply true power. Hence the expression (17) becomes

$$\begin{bmatrix} I_d \\ I_q \end{bmatrix} = \begin{bmatrix} I_{max} \\ 0 \end{bmatrix} \quad (17)$$

Where  $I_{max}$  is the maximum output current from the inverter. The error signal is developed by the expressions (18) and (19)

$$e_d(t) = I_d^{ref} - I_d(t) \quad (18)$$

$$e_q(t) = I_q^{ref} - I_q(t) \quad (19)$$

### 4.3. Designing of synchronous reference frame current controller

The current from the inverter  $I_{inv}$  and the voltage from the grid  $V_{grid}$  should be in-phase in order to apply the true power to the grid. Hence for this approach the d-q Synchronous frame current control is applied. An extra orthogonal phase voltage grid and inverter current are developed to transform into SRF from stationary reference frame because this control is used for the d-q Synchronous frame current control is applied. An extra orthogonal phase voltage grid and inverter current are developed to transform into SRF from stationary reference frame because this control is used for a single phase system instead of three phase system. It is very challenging task in single phase system to produce zero steady state error at grid frequency. SRF control helps to create two phases by creating an orthogonal pair which is shown in Fig 8. The PLL is used to trail the grid voltage phase angle. The inverter current  $I_a$  is used in order to generate its orthogonal pair  $I_\beta$ . The grid voltage  $V_{g\alpha}$  used to generate its orthogonal pair  $V_{g\beta}$  [25].

$$V_{g\alpha}(t) = V \cos(\omega t) \quad (11)$$

$$V_{g\beta}(t) = V \sin(\omega t) \quad (12)$$

Where  $V$  is the maximum voltage obtained from grid and  $\omega t$  is the phase angle generated using PLL. The inverter current  $I_a(t)$  and its orthogonal pair  $I_\beta(t)$  is given in the expression (13) and (14).  $\Phi$  is the inverter current phase angle [25].

$$I_\alpha(t) = I \cos(\omega t + \phi) \quad (13)$$

$$I_\beta(t) = I \sin(\omega t + \phi) \quad (14)$$

$I_d$  and  $I_q$  are obtained as a constant DC component with the help of the conversion from stationary rotating frame to synchronous rotating frame and this control action executes with the help of the PI controller.

$$\begin{bmatrix} I_d \\ I_q \end{bmatrix} = \begin{bmatrix} \cos \theta & \sin \theta \\ -\sin \theta & \cos \theta \end{bmatrix} \begin{bmatrix} I_\alpha \\ I_\beta \end{bmatrix} \quad (15)$$

By applying expressions (13), (14) in the above (15) expression where  $\omega t = \theta$ , we get

Where  $I_d^{ref}$  is obtained using the dc voltages from the boost converter, it is the reference current which develops the active power and supplied to the grid.  $I_q^{ref}$  is the reference current which develops the reactive power and is assumed to be zero. For the inverter in the d-q system the continuous time state equation relies upon the inverter model in the SRF controller coupling condition on the inverter side and is given in the expression (20) and (21)

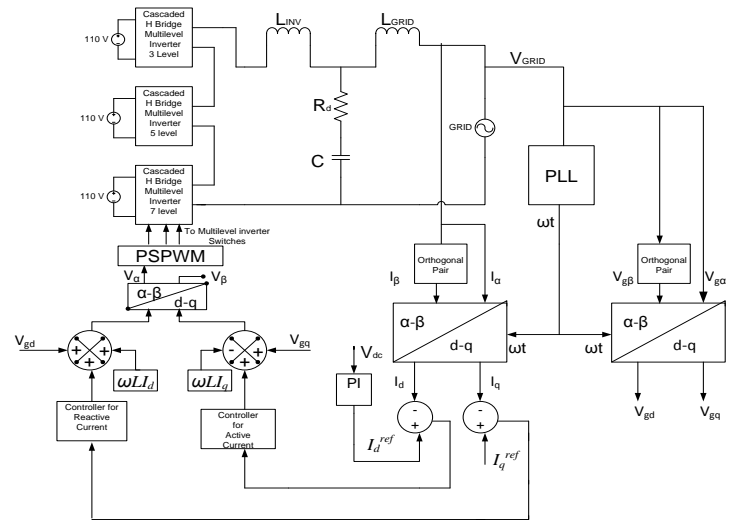


Fig. 8: Block Diagram for the D-Q SRF Current Control.

$$V_{id} = V_{gd} + R i_d + L \frac{di_d}{dt} - \omega L i_q \quad (20)$$

$$V_{iq} = L \frac{di_q}{dt} + V_{gq} + R i_q + \omega L i_d \quad (21)$$

The d and q decoupling condition on the controller side is given in the expression (22) and (23)

$$V_{id} = V_{gd} - \omega L i_q + \left[ k_p + \frac{k_i}{s} \right] (i_d^{ref} - i_d) \quad (22)$$

$$V_{iq} = V_{gq} + \omega L i_d + \left[ k_p + \frac{k_i}{s} \right] (i_q^{ref} - i_q) \quad (23)$$

From d-q to  $\alpha$ - $\beta$  conversion we get

$$\begin{bmatrix} V_\alpha \\ V_\beta \end{bmatrix} = \begin{bmatrix} \cos \omega t & -\sin \omega t \\ \sin \omega t & \cos \omega t \end{bmatrix} \begin{bmatrix} V_{id} \\ V_{iq} \end{bmatrix} \quad (24)$$

In the above expression  $V_\alpha$  is the reference signal for the Phase shifted Pulse with modulation (PSPWM).

#### 4.4. Designing of LCL filter

The inductance value in the converter side is designed to suppress the ripples that has been generated by the voltage source inverter. The inductor placed in the inverter side is estimated using the expression (25).  $V_{dc}$  is the dc voltage,  $f_{sw}$  is the switching frequency,  $I_{peak}$  is the amplitude of the current in grid. The filter capacitor is estimated using (26)

$$\frac{V_{dc}}{6.4 * f_{sw} * I_{peak}} \leq L_{INV} \leq \frac{V_{dc}}{2.4 * f_{sw} * I_{peak}} \quad (25)$$

$$C = \frac{0.05 * P_{grid}}{\omega_g * V_{GRID}^2} \quad (26)$$

Prated is the maximum power,  $\omega_g$  is the angular grid frequency and  $V_{GRID}$  is the RMS of the grid voltage. The inductor in the grid side value is estimated using the expression

$$L_{GRID} = r * L_{INV} \quad (27)$$

The percentage of the r factor, between  $L_{GRID}$  and  $L_{INV}$  is adopted as 0.5 to calculate the grid Inductance. The Parameter values for PV module and Inverter along with LCL values are given in Table 1. and Table 2.

**Table 1:** Parameters for the PV Panel

S. No	Components	Parameter for PV Module
1	Current at Short Circuit ( $I_{sc}$ )	8.7 A
2	Voltage at Open Circuit ( $V_{oc}$ )	22.8 V
3	Current at the Maximum ( $I_{mpp}$ )	8.2 A
4	Voltage at the Maximum ( $V_{mpp}$ )	18.4 V
5	Maximum Power ( $P_{max}$ )	150.88 W
6	Series Cells	60

**Table 2:** Parameters for the Inverter and LCL Filter

S. No	Components	Parameter for PV Module
1	Inverter side Inductor ( $L_{INV}$ )	3.76 mH
2	Grid side Inductor ( $L_{GRID}$ )	1.88 mH
3	Filter Capacitor Value (C)	1.362 $\mu$ F
4	Damping Resistor ( $R_d$ )	10 $\Omega$
5	Resonance frequency ( $f_{res}$ )	3632 Hz
6	Fundamental frequency	50 Hz
7	Switching frequency	5 kHz
8	DC Voltage ( $V_{dc}$ )	330 V
9	Grid Voltage ( $V_{GRID}$ )	230 V
10	Kp and Ki	4.58 and 0.02

### 5. Simulation results

The simulation results for the proposed system is discussed in this section. The overall simulation diagram with the subsystems is shown in the Fig.9.

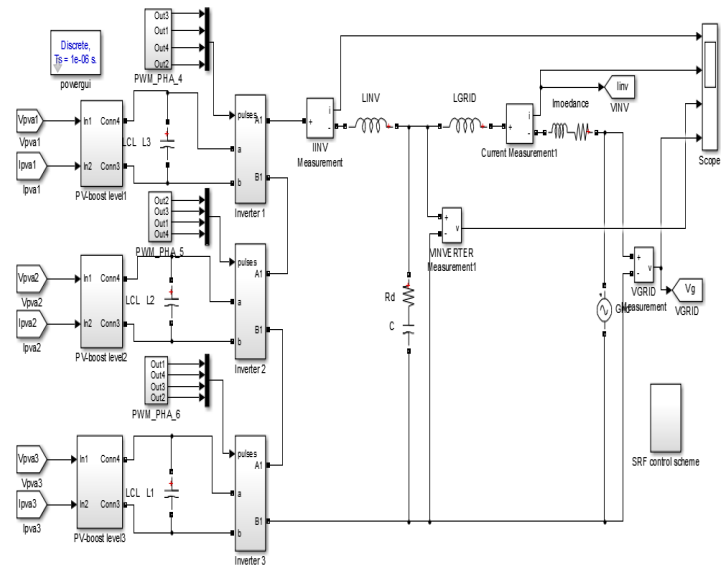


**Fig. 9:** Simulink Model for the Proposed System.

The output voltage and current of first pv and first boost is shown in Fig.10. and Fig.11. The inverter used in this proposed system is conventional cascaded H bridge inverter which has three separate dc sources hence three pv panels and three boost converters are connected in this system. The output voltage and current at 2nd PV is 18.98V and 7.712 A and 3rd PV is 18.97 V and 7.724 A. The V and I at the output of 2nd boost is 113.2 V and 1.264 A and 3rd boost V and I is 113.8V and 1.261 A respectively. Fig .12. And Fig.13 shows the current and Voltage after d-q transformations. Fig.14 and Fig.15 shows the active and reactive power of the grid and inverter side Fig.16 shows  $V_\alpha$  and  $V_\beta$  generated by the d-q method. Fig.17 shows the grid current and voltage are in phase. Fig.18 shows the THD of the grid current and is about 2.77%. Fig.19 and Fig.20 shows the THD Voltage of inverter side without Filter is of 20.20% and with filter is 0.41V.

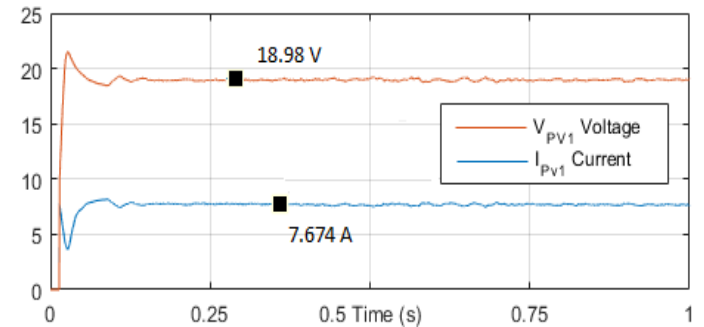


**Fig. 10:** Voltage and Current at the Output of the First PV.

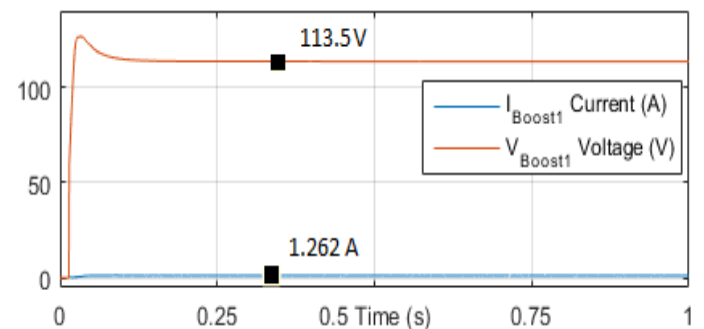


**Fig. 11:** Voltage and Current at the Output of the Boost.

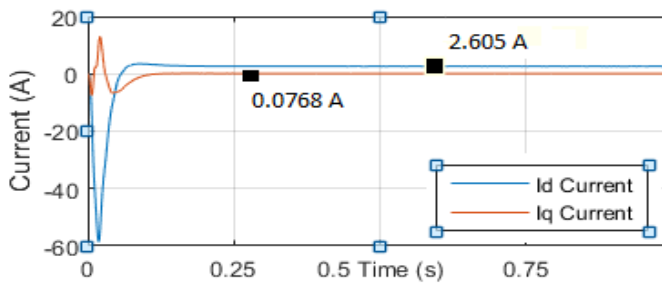


Fig. 12: D-Q SRF Control of the Inverter Current.

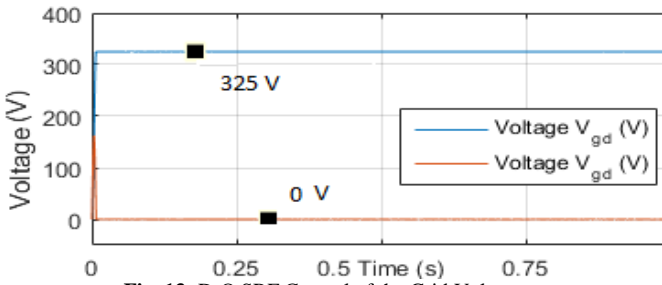


Fig. 13: D-Q SRF Control of the Grid Voltage.

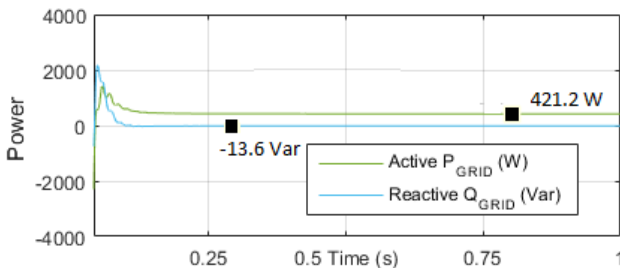


Fig. 14: Active and Reactive Power at the Grid Side.

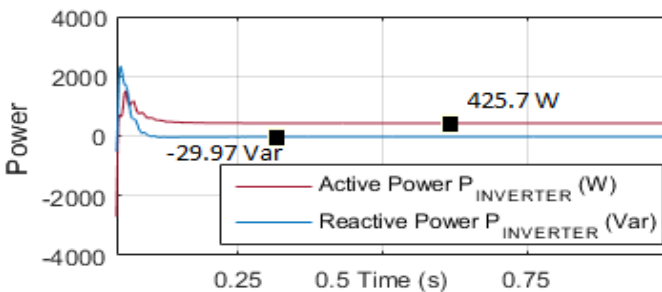


Fig. 15: Active and Reactive Power at the Inverter Side.

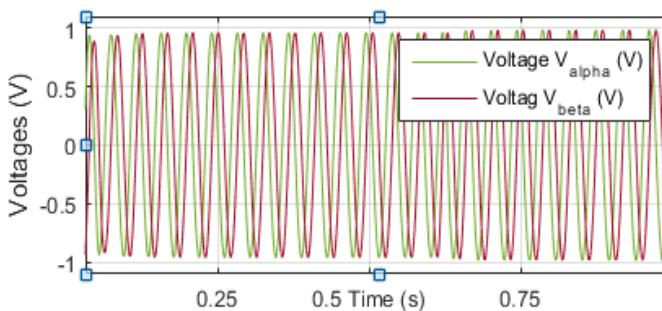


Fig. 16:  $V_{\alpha}$  and  $V_{\beta}$  Generated by the D-Q Method

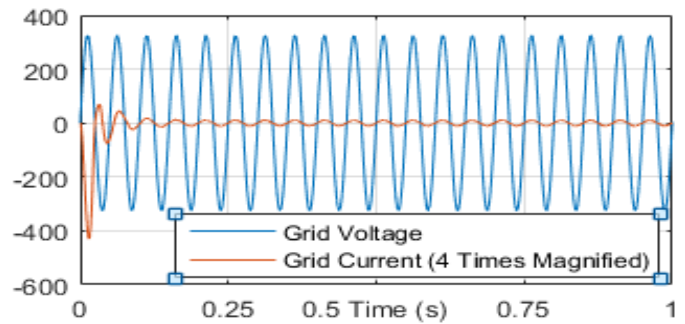


Fig. 17: Grid Voltage and Grid Current are in Phase.

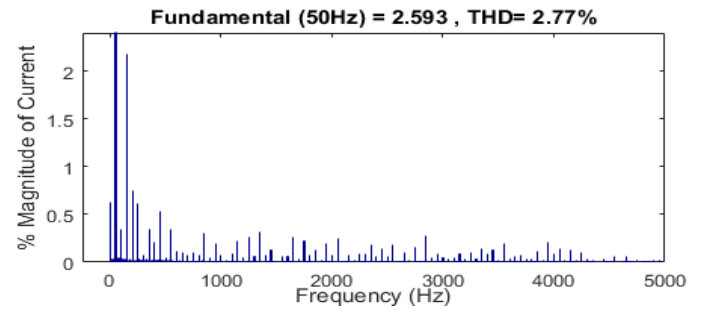


Fig. 18: THD Analysis for the Grid Current Using D-Q SRF.

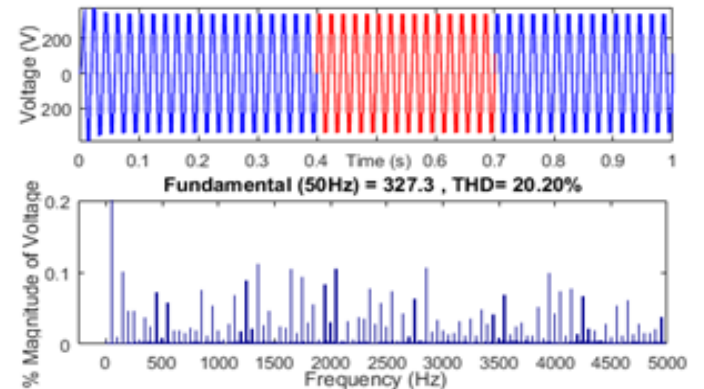


Fig. 19: THD Analysis for the Inverter Voltage without Filter.

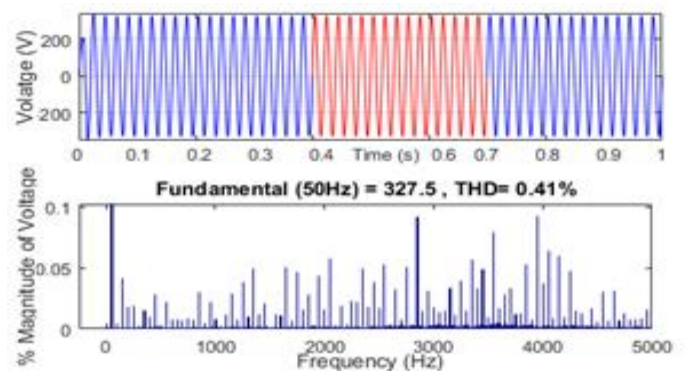


Fig. 20: THD Analysis for the Inverter Voltage with Filter.

## 6. Conclusion

The synchronous reference frame modelling using current control transformer less grid tie cascaded H bridge multilevel inverter using renewable source for single phase system is described. The proposed modeling is generated with LCL filter design. The rated power supplied by the solar panel is 452.64W. The power obtained at the grid side is about 421.2 W. Hence the efficiency of the proposed modelling is about 93% with the current controller method. The THD of the current supplied to the grid is 2.77% which satisfies the standard grid current value. The model is developed and analysed with the help of the MATLAB/Simulink tool.

## References

- [1] Enrique, J.M.; Andujar, J.M.; and Bohorquez, M.A A reliable, fast and low cost maximum power point tracker for photovoltaic applications. *Solar Energy*, 84, 79–89, 2010. <https://doi.org/10.1016/j.solener.2009.10.011>.
- [2] Liu, Y.H.; and Huang, J.W. A fast and low cost analog maximum power point tracking method for low power photovoltaic systems. *Solar Energy*, 85, 2771-2780.2011
- [3] M. G. Villalva, J. R. Gazoli, and E. Ruppert F., "Modeling and circuit based Simulation of photovoltaic arrays", *Power Electronics Conference, Bonito-Mato Grosso do Sui*, pp. 1244-1254, Sep. 2009.
- [4] Esram, T.; and Chapman, P.L. Comparison of photovoltaic array maximum power point tracking techniques. *IEEE Transactions on Energy Conversion*, 22, 439-449.2007
- [5] Safari, A.; and Mekhilef, S. Simulation and hardware implementation of incremental conductance MPPT with direct control method using cuk converter. *IEEE Transactions on Industrial Electronics*, 58(4), pp- 1154-1161.2011
- [6] Harini, Kancherla, and S. Syama. "Simulation and analysis of incremental conductance and Perturb and Observe MPPT with DC-DC converter topology for PV array." In *Electrical, Computer and Communication Technologies (ICECCT)*, 2015 IEEE International Conference on, pp. 1-5. IEEE, 2015. <https://doi.org/10.1109/ICECCT.2015.7225989>.
- [7] VS Kirthika Devi and S. G. Srivani. "Performance assessment of PV energy conversion system with Buck-Boost and Cuk converter for cascaded H-Bridge inverter." In *Power and Energy Systems: Towards Sustainable Energy (PESTSE)*, 2016 Biennial International Conference on, pp. 1-6. IEEE, 2016.
- [8] Liu, F.; Duan, S.; Liu, F.; Liu, B.; and Kang, Y. A variable step size INC MPPT method for PV systems. *IEEE Transactions on Industrial Electronics*, 55(7), 2622-2628. (2008). <https://doi.org/10.1109/TIE.2008.920550>.
- [9] Mohan, Ned, and Tore M. Undeland. *Power electronics: converters, applications, and design*. John Wiley & Sons, 2007.
- [10] Hart, Daniel W. *Power electronics*. Tata McGraw-Hill Education, 2011.
- [11] Umanand, L. "Power electronics essentials and applications." 1sted. New York, NY, Wiley Publishers 2009.
- [12] Rolim, Lus Guilherme Barbosa, Diogo Rodrigues da Costa Jr, and M.Aredes. "Analysis and software implementation of a robust synchronizing PLL circuit based on the pq theory." *IEEE Transactions on Industrial Electronics* 53, no.6 pp-1919-1926, 2008.
- [13] Zhang, Qi, Xiang-Dong Sun, Yan-Ru Zhong, Mikihiko Matsui, and Bi-Ying Ren. "Analysis and design of a digital phase-locked loop for single-phase grid-connected power conversion systems." *IEEE Transactions on Industrial Electronics* 58, no. 8, pp- 3581-3592. 2011
- [14] Zmood, Daniel Nahum, and Donald Grahame Holmes. "Stationary frame current regulation of PWM inverters with zero steady-state error." *IEEE Transactions on power electronics* 18, no. 3: 814-822. 2003 <https://doi.org/10.1109/TPEL.2003.810852>.
- [15] Franceschini, Giovanni, Emilio Lorenzani, Carla Tassoni, and Alberto Bellini. "Synchronous reference frame grid current control for single-phase photovoltaic converters." In *Industry Applications Society Annual Meeting, 2008. IAS'08*. IEEE, pp. 1-7. IEEE, 2008. <https://doi.org/10.1109/08IAS.2008.74>.
- [16] Wen, Bo, Dushan Boroyevich, Rolando Burgos, Paolo Mattavelli, and Zhiyu Shen. "Analysis of DQ small-signal impedance of grid-tied inverters." *IEEE Transactions on Power Electronics* 31, no. 1: 675-687. 2016 <https://doi.org/10.1109/TPEL.2015.2398192>.
- [17] Malinowski, Mariusz, K. Gopakumar, Jose Rodriguez, and Marcelo A. Perez. "A survey on cascaded multilevel inverters." *IEEE Transactions on industrial electronics* 57, no. 7: 2197-2206. 2010 <https://doi.org/10.1109/TIE.2009.2030767>.
- [18] Tolbert, Leon M., Fang Zheng Peng, and Thomas G. Habetler. "Multilevel PWM methods at low modulation indices." *IEEE Transactions on power electronics* 15, no. 4 pp.719-725. 1992 <https://doi.org/10.1109/63.849042>.
- [19] Carrara, Giuseppe, Simone Gardella, Mario Marchesoni, Raffaele Salutati, and Giuseppe Sciotto. "A new multilevel PWM method: A theoretical analysis." *IEEE Transactions on power electronics* 7, no. 3 pp-497-505. 1992
- [20] Wu, Bin, and Mehdi Narimani. *High-power converters and AC drives*. Vol. 59. John Wiley & Sons, 2017. <https://doi.org/10.1002/9781119156079>.
- [21] V S Kirthika Devi and S. G. Srivani. "Modified phase shifted PWM for cascaded H bridge multilevel inverter." In *Advances in Electrical, Electronics, Information, Communication and Bio-Informatics (AEEICB)*, 2017 Third International Conference on, pp. 89-94. IEEE, 2017.
- [22] Farhadi Kangarlu, Mohammad, Ebrahim Babaei, and Frede Blaabjerg. "An LCL-filtered single-phase multilevel inverter for grid integration of PV systems." *Journal of Operation and Automation in Power Engineering* 4, no. 1: 54-65. 2016
- [23] González, Roberto, Jess Lopez, Pablo Sanchis, and Luis Marroyo. "Transformerless inverter for single-phase photovoltaic systems." *IEEE Transactions on Power Electronics* 22, no. 2: 693-697. 2007 <https://doi.org/10.1109/TPEL.2007.892120>.
- [24] González, Roberto, Eugenio Gubía, Jesús López, and Luis Marroyo. "Transformerless single-phase multilevel-based photovoltaic inverter." *IEEE Transactions on Industrial Electronics* 55, no. 7: 2694-2702. 2008 <https://doi.org/10.1109/TIE.2008.924015>.
- [25] Remus Teodorescu, Marco Liserre and Pedro Rodriguez Grid Converters for Photovoltaic and Wind Power Systems", IEEE and John Wiley & Sons, Ltd, 2 ISBN “: 978-0-470-05751-3. 2011.